Cardiovascular, skeletal, and renal defects in mice with a targeted disruption of the *Pkd1* gene

Catherine Boulter*, Sharon Mulroy*†, Sandra Webb‡, Stewart Fleming§, Kevin Brindle¶, and Richard Sandford†‖

Departments of *Genetics, ¶Biochemistry, and †Medical Genetics, University of Cambridge, Cambridge CB2 1TN, United Kingdom; ‡Department of Anatomy and Developmental Biology, St. George's Hospital Medical School, London 5W17 ORE, United Kingdom; and §Department of Molecular and Cellular Pathology, University of Dundee, Dundee DD195Y, United Kingdom

Edited by Oliver Smithies, University of North Carolina at Chapel Hill, Chapel Hill, NC, and approved August 8, 2001 (received for review April 18, 2001)

Autosomal dominant polycystic kidney disease (ADPKD) is characterized by cyst formation in the kidney, liver, and pancreas and is associated often with cardiovascular abnormalities such as hypertension, mitral valve prolapse, and intracranial aneurysms. It is caused by mutations in *PKD1* or *PKD2*, encoding polycystin-1 and -2, which together form a cell surface nonselective cation ion channel. *Pkd2*−/− mice have cysts in the kidney and pancreas and defects in cardiac septation, whereas *Pkd1*^{del34} −/− and *Pkd1*^{L} −/− mice have cysts but no cardiac abnormalities, although vascular fragility was reported in the latter. Here we describe mice carrying a targeted mutation in *Pkd1* (*Pkd1*$^{del17–21\beta geo}$), which defines its expression pattern by using a *lacZ* reporter gene and may identify novel functions for polycystin-1. Although *Pkd1*$^{del17–21\beta geo}$ +/− adult mice develop renal and hepatic cysts, *Pkd1*$^{del17–21\beta geo}$ −/− embryos die at embryonic days 13.5–14.5 from a primary cardiovascular defect that includes double outflow right ventricle, disorganized myocardium, and abnormal atrio-ventricular septation. Skeletal development is also severely compromised. These abnormalities correlate with the major sites of *Pkd1* expression. During nephrogenesis, *Pkd1* is expressed in maturing tubular epithelial cells from embryonic day 15.5. This expression coincides with the onset of cyst formation in *Pkd1*^{del34} −/−, *Pkd1*^{L} −/−, and *Pkd2*−/− mice, supporting the hypothesis that polycystin-1 and polycystin-2 interact *in vivo* and that their failure to do so leads to abnormalities in tubule morphology and function.

Autosomal dominant polycystic kidney disease (ADPKD) is a common inherited disorder that affects 1 in 800 people and accounts for ≈8% of patients with end-stage renal failure. It is characterized by the formation of multiple cysts in the kidneys and liver and, less frequently, in the pancreas. Cardiovascular abnormalities including hypertension, mitral valve prolapse, and intracranial aneurysms are also frequently recognized. Extensive characterization of the cellular defects in cyst-lining epithelial cells derived from kidneys affected by ADPKD and from a variety of rodent models of renal cystic disease has demonstrated generalized abnormalities in cell proliferation, differentiation, and apoptosis (1–3). More specific defects in cell polarity and extracellular matrix production are also seen and have been implicated directly in the process of cyst formation (4, 5). However, the primary events that give rise to this cystic phenotype have not been elucidated.

The cloning of *PKD1* and *PKD2*, the genes mutated in almost all cases of ADPKD, has provided the opportunity to investigate the molecular basis of cyst formation and develop appropriate model systems to study the functions of their protein products, polycystin-1 and -2. Both are predicted to be polytopic membrane proteins, with polycystin-1 having a large predicted extracellular region comprising multiple discrete domains while polycystin-2 has homology to ion channels (6, 7). An interaction mediated by the C-terminal regions of both proteins results in the formation of calcium-permeable nonselective cation channels *in vitro*, suggesting that extracellular signals can be transduced by the polycystin complex to regulate diverse cellular processes (8). Indeed, the cytoplasmic tail of polycystin-1 has been shown to activate several signal transduction pathways (9, 10), whereas Madin-Darby canine kidney cells transfected with *PKD1* are resistant to apoptosis and undergo spontaneous tubulogenesis (11). The nature of the extracellular signals or protein ligands that activate polycystin-1 signaling have not been determined.

The formation of a polycystin complex suggests that *Pkd1* and *Pkd2* should have considerable overlap in their expression patterns, and detailed analysis of the cellular and subcellular distribution has been performed. Expression of polycystin-2 has been defined in renal tubular epithelial cells with widespread expression reported in other tissues including the heart and vasculature (12–14). Unfortunately, considerable differences have been reported in the expression pattern of polycystin-1 by using both antibodies directed against different epitopes and RNA *in situ* hybridization (15–23). This has made meaningful comparisons of *Pkd1* and *Pkd2* expression difficult.

Mice carrying targeted mutations in *Pkd1* and *Pkd2* or a *PKD1* transgene have been reported (24–28). They all have renal cysts, suggesting that alterations in the level of polycystin-1 lead to cyst formation. Both *Pkd1*^{del34} −/− and *Pkd1*^{L} −/− mice develop renal, hepatic, and pancreatic cystic disease. However *Pkd1*^{L} −/− embryos also develop gross edema and s.c. hemorrhage, which may be caused by a defect in vascular wall integrity (24). Unlike these models, *Pkd2* mutant mice also have major defects in cardiac development manifested by septal abnormalities in addition to the cystic phenotype (27).

Here we describe a mouse model of ADPKD that allows the accurate description of *Pkd1* expression by using a *lacZ* reporter gene and identifies a major function for polycystin-1 in cardiovascular and skeletal development in addition to its role in embryonic and adult kidney.

Materials and Methods

Pkd1 Gene Targeting. A 14-kb mouse genomic fragment containing *Pkd1* exons 15–33 was isolated from a λ2001 129/Sv genomic DNA library derived from the CCB embryonic stem (ES) cell line (constructed by A. Smith) by screening with a human *PKD1* cDNA probe. To construct the targeting vector (p*Pkd1*$^{del17–21\beta geo}$), a 6.5-kb *Xba*I fragment (with one *Xba*I site derived from the λ2001 polylinker) containing exons 15–21 was cloned into pBS (Stratagene). A 1.5-kb *Hin*dIII–*Xba*I fragment including exons 17–21 was deleted and replaced with a promotorless cassette containing a 5′ donor *engrailed-2* intron and splice acceptor site, an internal ribosome entry site (IRES)

This paper was submitted directly (Track II) to the PNAS office.

Abbreviations: ADPKD, autosomal dominant polycystic kidney disease; ES, embryonic stem; IRES, internal ribosome entry site; WT, wild type; E*n*, embryonic day *n*; *βgeo*, *lacZ-neomycin*^{R} fusion gene; X-Gal, 5-bromo-4-chloro-3-indolyl-β-D-galactoside; DORV, double outlet right ventricle.

‖To whom reprint requests should be addressed: Addenbrooke's Hospital, Cambridge, CB2 2XY, UK. E-mail: rns13@cam.ac.uk.

The publication costs of this article were defrayed in part by page charge payment. This article must therefore be hereby marked "*advertisement*" in accordance with 18 U.S.C. §1734 solely to indicate this fact.

www.pnas.org/cgi/doi/10.1073/pnas.211191098

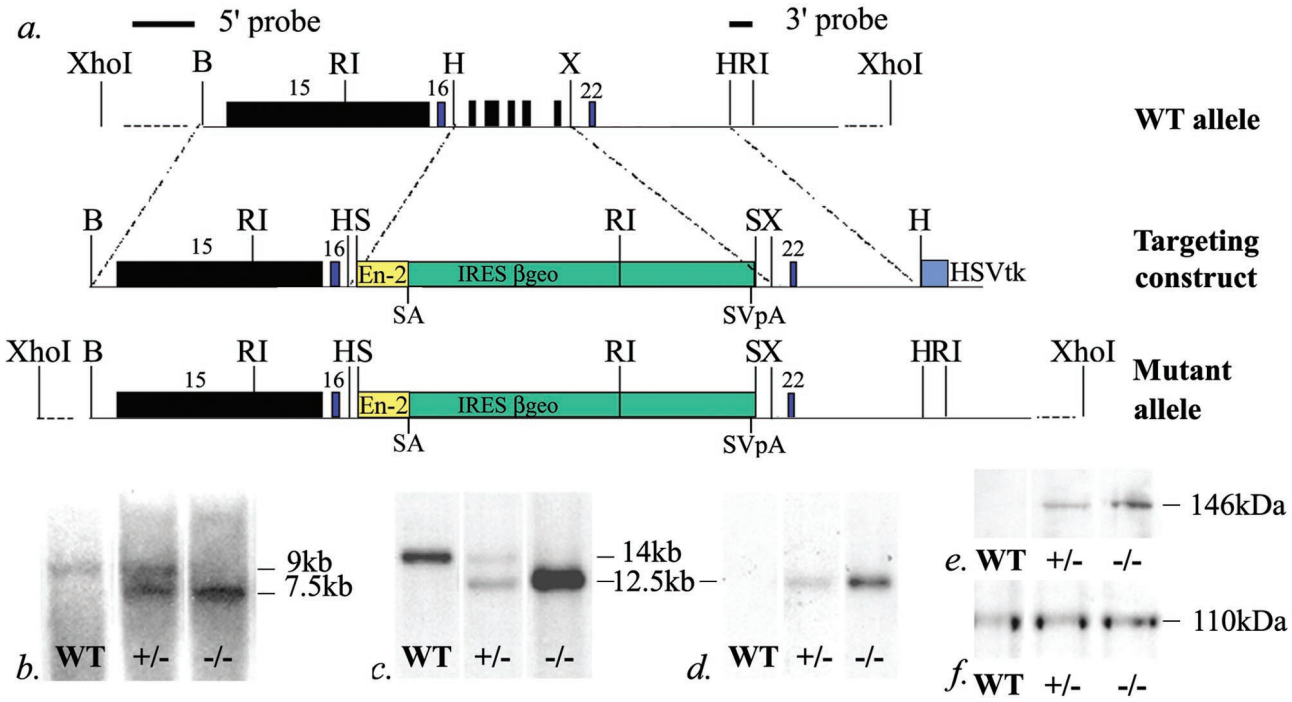

Fig. 1. Generation of a targeted disruption of *Pkd1*. (*a*) *Pkd1* exons 17–21 were replaced with a *lacZ-neomycin*^{R} fusion gene (βgeo) located downstream of an *engrailed-2* gene donor intron (En-2) and splice acceptor site (SA), an IRES, and upstream of a simian virus 40 polyadenylation signal (SVpA). The positions of the 5′ and 3′ external probes are indicated. HSVtk, herpes simplex virus thymidine kinase gene; B, *Bam*HI; RI, *Eco*RI; H, *Hin*dIII; X, *Xba*I; S, *Sal*I. (*b*) A Southern blot of *Eco*RI-digested DNA from a cross of *Pkd1*$^{del17–21βgeo}$ +/− mice hybridized with an external 3′ probe showing the WT (+/+) (9 kb) and mutant (7.5 kb) alleles; this result was confirmed with the 5′-external probe (data not shown). (*c*) Northern analysis using a *Pkd1* exon 15 probe demonstrated the ≈14-kb *Pkd1* transcript in WT (+/+) and *Pkd1*$^{del17–21βgeo}$ +/− embryos and the predicted 12.5-kb mutant transcript in *Pkd1*$^{del17–21βgeo}$ +/− and −/− embryos; different intensities between RNA samples reflected different RNA loading are shown. (*d*) A *neo*^{R} probe confirmed the presence of the 12.5-kb mutant transcript in *Pkd1*$^{del17–21βgeo}$ +/− and −/− embryos. (*e*) Independent translation of the βgeo gene was demonstrated by using an anti-β-galactosidase antibody to detect the predicted 146-kDa β-galactosidase-neomycin fusion protein. (*f*) Levels of polycystin-2 (110 kDa) were unaltered in *Pkd1*$^{del17–21βgeo}$ +/− and −/− E12.5 embryos compared with WT (+/+) littermates.

coupled to a *lacZ-neomycin*^{R} fusion gene (*βgeo*), and a 3′-simian virus 40 polyadenylation site (29). The 3′ region of homology was cloned as a 5.8-kb *Xba*I–*Hin*dIII fragment, and a phosphoglycerate kinase promoter-herpes simplex virus thymidine kinase gene (HSVTK) negative selection cassette was ligated downstream. The targeting construct is shown in Fig. 1. *Not*I-linearized p*Pkd1*$^{del17–21βgeo}$ was electroporated into CCB ES cells. G418-resistant clones were selected and screened by Southern blotting using *Eco*RI-cut genomic DNA and the 3′ probe. Of 266 ES cell clones screened, 11 clones containing the correctly targeted mutant allele (*Pkd1*$^{del17–21βgeo}$) were identified. Chimeric mice were generated by C57/Bl6 blastocyst injection and germline transmission determined by glucose phosphate isomerase assay (30). Chimeric males were bred to 129/Sv females, and offspring were genotyped by Southern blotting (Fig. 1*b*) and PCR. PCR primers were directed against the IRES and *Pkd1* exons 18 and 19 (sequences and PCR parameters are available on request). Wild type (WT) animals were positive for the exon 18–19 PCR and negative for the IRES PCR; *Pkd1*$^{del17–21βgeo}$ +/− animals were positive for both, and *Pkd1*$^{del17–21βgeo}$ −/− animals were positive only for the IRES PCR.

Analysis of RNA and Protein. Total RNA was prepared from E12.5 embryos by first grinding snap frozen embryos in liquid nitrogen and then by using the method of Chomczynski and Sacchi (31). Northern blot analysis of 20 μg of total RNA was carried out according to standard protocols by using *Pkd1* exon 15 or the *neo*^{R} gene as probes. Total protein (10–15 μg) from whole mouse embryo homogenates was used to detect polycystin-2 and β-galactosidase expression by Western blot analysis under reducing conditions. The primary antibodies used were PKD2-CFP (12) at a dilution of 1:1,000 and a mouse monoclonal antibody against β-galactosidase at 1:5,000 dilution (Promega catalog number Z3781).

Staining for β-Galactosidase Activity in Tissues and Frozen Sections. Staining for β-galactosidase activity was carried out according to published protocols (32). Fixation and staining times varied depending on tissue and sample size. Samples were postfixed in 4% paraformaldehyde in PBS and stored in 70% EtOH at 4°C. Samples were transferred to 70% methanol, dehydrated through graded methanols, and cleared in benzylalcohol/benzylbenzoate (1:1) before photography. Frozen sections were counterstained with nuclear fast red before permanent mounting.

Histological and Skeletal Analysis. Tissues and embryos for histological analysis were fixed overnight in 4% paraformaldehyde in PBS and stored in 70% ethanol before paraffin embedding. Paraffin sections of 6 μm were cut and stained with hematoxylin and eosin. Skeletal preparations and cartilage staining were carried out as described (32).

Nuclear Magnetic Resonance Imaging. Magnetic resonance images were acquired at a magnetic field of 9.4 T (400-MHz proton frequency) by using an unshielded gradient set and a 25 mm diameter ^{1}H probe (Varian Ltd). The images were acquired by using a spin echo pulse sequence (time to echo = 60 msec, time to return = 2 sec) with 256 phase-encode increments and 16

transients per increment. The echoes were acquired into 512 data points, and the data set zero was filled to 1,024 × 1,024 data points before two-dimensional Fourier transformation. The slice thickness was 500 μm, and the in-plane resolution was 78 × 78 μm.

Results

Generation of Knockout Mice Carrying a Truncating Mutation in *Pkd1* and an Inserted *lacZ* Gene. We have generated mice carrying a truncating mutation in the *Pkd1* gene ($Pkd1^{del17–21\beta geo}$) by using gene targeting to replace exons 17–21 of the *Pkd1* gene with a *lacZ-neomycin* fusion gene (*βgeo*) downstream of a splice acceptor site and an IRES (Fig. 1 *a* and *b*) (29). The resulting transcript, containing the first 16 exons of *Pkd1* spliced to *βgeo*, is predicted to encode a truncated form of polycystin-1, which includes only the extracellular domains up to and including the PKD repeats, and thus represents a common class of mutation found in ADPKD patients (33). Northern analysis demonstrated expression of the expected 12.5-kb *Pkd1-βgeo* fusion transcript and loss of the WT 14.5-kb *Pkd1* transcript in $Pkd1^{del17–21\beta geo}$ −/− E12.5 embryos (Fig. 1 *c* and *d*). Western blotting confirmed that the IRES was used efficiently to produce a β-galactosidase-neomycin fusion protein (Fig. 1*e*) and indicated that the expression level of *Pkd2* was unaffected in $Pkd1^{del17–21\beta geo}$ +/− and −/− E12.5 embryos (Fig. 1*f*). The efficient translation of *βgeo* mRNA allowed *Pkd1* expression to be visualized by staining with X-Gal and correlations to be made with the phenotype of mutant mice.

Kidney and Liver Cysts in $Pkd1^{del17–21\beta geo}$ Heterozygotes and Expression of *Pkd1*. Microscopic renal cysts were observed in ≈50% of $Pkd1^{del17–21\beta geo}$ +/− mice analyzed before 9 months of age (n = 15) and were detected as early as 3 months, with occasional macroscopic cysts seen in animals of 4–19 months (n = 8/18). Cysts arose throughout the nephron and were often lined with hyperplastic cells or apoptotic cells (Fig. 2 *a* and *b*). X-Gal staining of kidneys from adult $Pkd1^{del17–21\beta geo}$ heterozygotes revealed activity of the *Pkd1* promoter in cyst-lining epithelia (Fig. 2*e*) but no significant up-regulation of the mutant allele compared with normal tubule epithelia. Low levels of *Pkd1* expression were detected throughout the nephron, except in podocytes, with the highest levels seen in the medullary and papillary collecting ducts, ureter, and renal vessels (Fig. 2 *b–d*). All WT tissues were negative or showed only weak background staining with X-Gal.

In addition to renal cysts, liver and pancreatic cysts are seen in ADPKD patients. *Pkd1* was expressed at low levels in the pancreatic ducts and intrahepatic bile ducts but not in hepatocytes (Fig. 3*a*). Liver cysts were found occasionally in $Pkd1^{del17–21\beta geo}$ heterozygotes from 19 months of age.

***Pkd1* Is Expressed in Maturing Tubule Epithelial Cells During Nephrogenesis.** During early metanephric development, up to E15.5, *Pkd1* expression was seen only in renal vessels and weakly in uninduced and induced mesenchyme (from E13.5), with the ureteric bud, comma, and S-shaped bodies negative (Fig. 2*g*). This is consistent with the observation that renal development of $Pkd1^{del17–21\beta geo}$ −/− embryos was normal until their deaths at E13.5-E14.5. From E15.5 to E18.5, *Pkd1* expression was increased dramatically in mesenchymal cells and endothelial cells in the nephrogenic zone and most significantly in the differentiating tubules of the nephron and collecting duct system (Fig. 2 *h–j*). No podocyte staining was seen. This correlates well with the time point at which cysts first arise in kidneys of $Pkd1^{del34}$ −/− and $Pkd1^{L}$ −/− embryos, suggesting that in the absence of functional polycystin-1 further development of tubule epithelial cells is impaired, and this results in cyst formation.

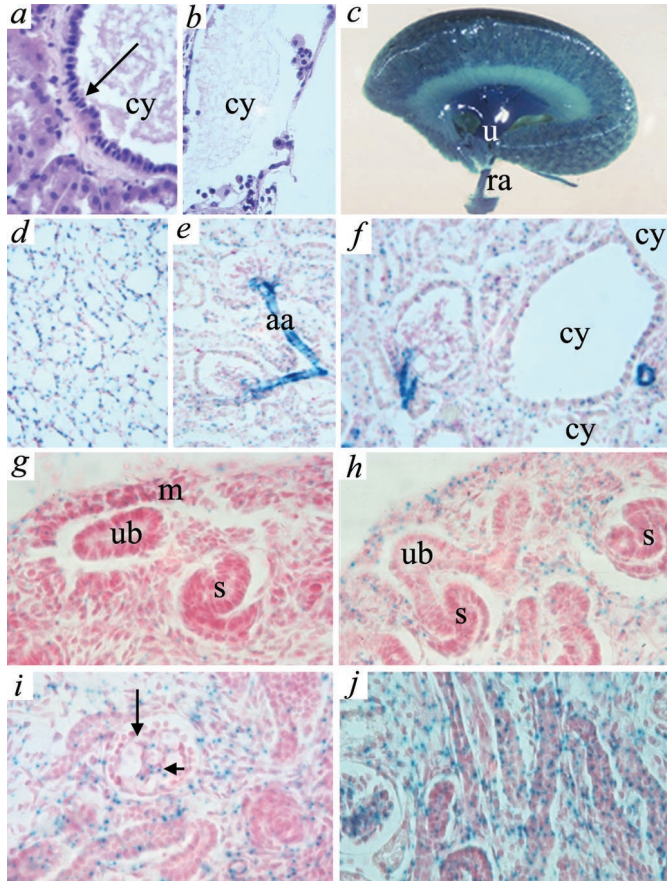

Fig. 2. Renal cysts and *Pkd1* expression in embryonic and adult kidneys of $Pkd1^{del17–21\beta geo}$ +/− mice demonstrated by using X-Gal staining. Renal cysts (cy) in $Pkd1^{del17–21\beta geo}$ +/− were lined with hyperplastic epithelial cells (*a*, arrowed) or cells with pyknotic apoptotic nuclei (*b*, ×60). (*c*) Whole-mount X-Gal staining of adult kidney. (*d-f*) Adult kidney frozen sections (×40). Expression is seen in all medullary collecting ducts (*d*), glomerular parietal, proximal and distal tubule epithelial cells (*e*), and in cystic epithelia (*f*). Strong staining of the afferent arterioles (aa) and other vascular structures was seen also. (*g-j*) *Pkd1* expression in $Pkd1^{del17–21\beta geo}$ +/− embryos during nephrogenesis (×60): *g*, E13.5; *h* and *i*, E15.5; *j*, E18.5. Expression is confined to mesenchyme (m) and maturing tubules. ub, ureteric bud; s, S-shaped body; long arrow, podocytes; short arrow, endothelium.

***Pkd1* Is Expressed Highly Throughout the Cardiovascular System.** Cardiovascular abnormalities are a major feature of ADPKD and include cerebral aneurysms, hypertension, and cardiac valvular defects (34). X-Gal staining of $Pkd1^{del17–21\beta geo}$ +/− adult tissues revealed high levels of *Pkd1* expression throughout the heart. Expression was highest in the aortic outflow tract and atrial appendages (Fig. 3*b*) and in the endothelial and vascular smooth muscle cells of the major vessels including the aorta (Fig. 3 *b* and *c*) and intracranial arteries (Fig. 3*d*), a site of aneurysm formation in ADPKD patients. In the embryonic cardiovascular system, *Pkd1* expression was detected at E9.5 in the aorta and later in all of the major vessels (Fig. 3*e*); from E10.5, all the structures of the heart were positive, with the highest expression in the outflow tracts, endocardial cushions and valve leaflets, and lower levels in the myocardium (Fig. 3*f*). This expression pattern suggested a role for polycystin-1 in cardiovascular development, a hypothesis supported by the phenotype of $Pkd1^{del17–21\beta geo}$ −/− embryos.

Abnormal Cardiovascular Development in $Pkd1^{del17–21\beta geo}$ Homozygote Embryos. $Pkd1^{del17–21\beta geo}$ −/− embryos died at E13.5-E14.5 with multiple developmental abnormalities. Progressive edema

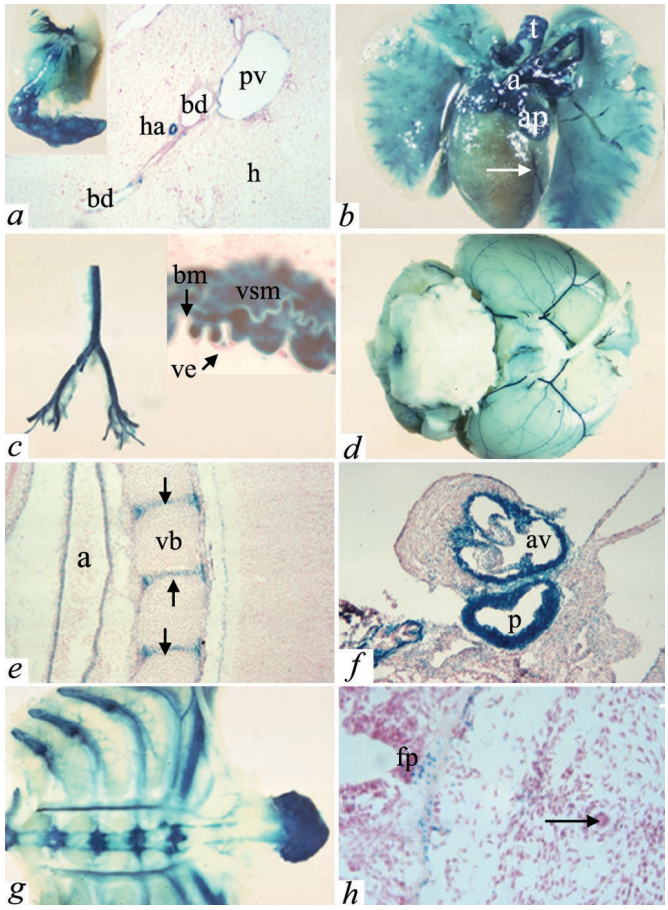

Fig. 3. Expression of *Pkd1* in nonrenal adult and embryonic tissues. (*a*) Adult liver [bd, bile ducts; ha, hepatic artery; pv, portal vein; h, hepatocytes (×10)]. (*Inset*) Whole-mount staining of gall bladder. (*b*) Adult heart. *Pkd1* was expressed strongly in the aortic outflow tract (a), atrial appendages (ap), and major coronary vessels (arrow). The cartilage rings of the trachea (t) and bronchi and vessels in the lung are also positive. (*c*) Dissected adult aorta. (*Inset*) Frozen section adult aorta (×40). *Pkd1* is expressed in vascular smooth muscle cells (vsm) and vascular endothelial cells (ve) separated by vascular basement membrane (bm). (*d*) Intracranial arteries. (*e* and *f*) *Pkd1* expression in the embryonic cardiovascular system. (*e*) Aorta (a) at E14.5. The cartilage of the developing vertebral bodies (vb) and intervertebral discs (arrows) are also positive (×10). (*f*) E18.5 cardiac outflow tract (p, pulmonary artery; av, aortic valve), (×20). (*g*) Whole-mount staining of sternum and ribs. Note also strong staining in vessels. (*h*) E11.5 floor plate (fp) and notochord (arrow) are sites of *Pkd1* expression (×40).

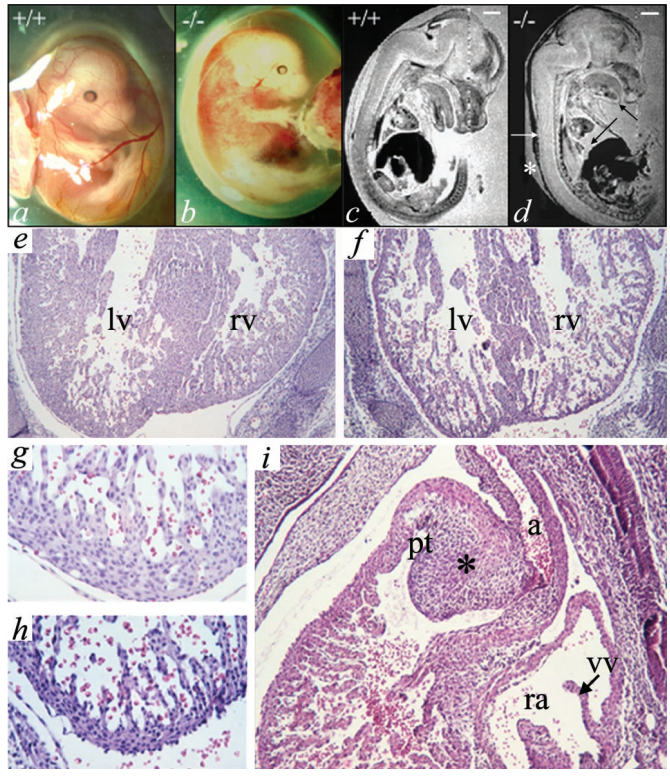

Fig. 4. Abnormal cardiovascular development in *Pkd1*$^{del17–21\beta geo}$ −/− embryos. (*a–d*) *Pkd1*$^{del17–21\beta geo}$ −/− embryos at E13.5 (*b* and *d*) were edematous and hemorrhagic compared with littermate controls (*a* and *c*). Magnetic resonance imaging demonstrated the marked edema (*), subcutaneous hemorrhage (white arrow), pericardial effusions (long black arrow), and abnormal craniofacial development (short black arrow) of *Pkd1*$^{del17–21\beta geo}$ −/− embryos (*d*) (scale bar, 1 mm). Hematoxylin/eosin staining of sagittal sections of E13.5 embryos showed hemorrhagic effusion and disorganization of the myocardial wall and ventricular septum in *Pkd1*$^{del17–21\beta geo}$ −/− embryos (*f* and *h*) but not in WT littermates (*e* and *g*). lv, left ventricle; rv, right ventricle. *e* and *f*, ×10; *g* and *h*, ×40. (*i*) Transverse section showing the heart of a *Pkd1*$^{del17–21\beta geo}$ −/− embryo at E13.5 showing a double outlet right ventricle (DORV) with the large dysplastic cushion mass forming the outlet septum (rv, right ventricle; ra, right atrium; pt, pulmonary trunk; a, aorta; vv, venous valves of the right atrium; *, outlet septum) (×10).

and focal hemorrhage suggested an underlying cardiovascular defect (Fig. 4 *b* and *d*). Histological examination revealed hemorrhagic pericardial effusion, disorganized myocardial trabeculation, and thinning of the myocardial wall. Other abnormalities seen included atrial and ventricular septal defects as well as DORV (Fig. 4 *e–i*; Table 1). Two animals with DORV also had a common atrio-ventricular junction with the atrial septum fused to the atrial aspect of the unfused atrio-ventricular cushions. The endocardial cushions and the cushion mass forming the outlet septum were dysplastic, appearing to be larger than normal (Fig. 4*i*).

Expression of *Pkd1* in Embryonic and Adult Cartilage and Disruption of Bone Development in *Pkd1*$^{del17–21\beta geo}$ Homozygote Embryos. Although no characteristic pattern of skeletal abnormality is recognized in ADPKD, an association with a Marfanoid habitus has been suggested (35). We have found high levels of *Pkd1* expression in adult cartilage (Fig. 3*f*). During embryogenesis, *Pkd1* is expressed in differentiating cartilage and somites and earlier in the notochord and floor plate, which are involved in somite development (Fig. 3 *e* and *h*). This pattern suggests a potential role for polycystin-1 in formation of the axial skeleton and in cartilage differentiation. Indeed, skeletal development was compromised severely in *Pkd1*$^{del17–21\beta geo}$ −/− embryos. Skeletal preparations of E12.5 and E13.5 embryos revealed that both the axial skeleton and long bones were abnormal (Fig. 5). The structure and organization of the vertebrae were disrupted, and the spines of all homozygotes analyzed were curved and twisted ($n = 4$). Compared with WT controls, the long bones were shorter and smaller in diameter, with splaying of the radius and ulna, and histological sectioning revealed that cartilage differentiation was delayed (data not shown). Defects were seen also in neural crest-derived tissues in the head, including Meckle's cartilage, consistent with the expression pattern of *Pkd1* in neural crest cells and their derivatives (20).

Discussion

The *Pkd1*$^{del17–21\beta geo}$ −/− mice described here reveal important new roles for polycystin-1 in cardiovascular and skeletal development. This phenotype is different from that of the previously reported *Pkd1* mutant mice, which die later in gestation and

Table 1. Abnormal cardiac development in *Pkd1*$^{del17–21\beta geo}$ −/− mice

Embryo	1	2	3	4	5	6	7	8	9	10	11	12
Gestation (E)	12.5	12.5	12.5	12.5	13	13	13	13	13	14	14.5	14.5
Edema			+	+	+	+	+	+	+	+	+	+
Normal heart					+							
DORV	+	+		+			+	+				
Myocardial disorganization			+	+		+	+		+	+	+	+
Common AV junction							+	+				

have no reported cardiac or skeletal defects, indicating that the site of mutation in *Pkd1* may influence the phenotype. The *Pkd1*$^{del17–21\beta geo}$ +/− mice also allow a detailed and accurate description of *Pkd1* expression, which largely agrees with RNA *in situ* hybridization studies (20, 21) and clarifies much of the conflicting immunolocalization data (15–18, 22, 23, 36–38).

Previous data based on immunohistochemistry and *in vitro* organ culture systems have suggested a role for polycystin-1 in ureteric bud growth and branching during kidney development (23, 39, 40). This article, however, demonstrates that polycystin-1 does not play a major role in early nephrogenesis. In agreement with RNA *in situ* hybridization data (20), *Pkd1* expression during early nephrogenesis is limited, with weak expression in uninduced and induced mesenchyme and no expression in the ureteric bud and comma and S-shaped bodies. Consistent with this observation, early nephrogenesis is normal in this and other *Pkd1* mutant embryos (24, 25). Instead, our data suggest a role for polycystin-1 in tubule maturation with induction of *Pkd1* expression in maturing tubule epithelial cells from E15.5. This timing coincides with the basolateral localization of polycystin-2 in tubule epithelial cells and the onset of cyst formation in *Pkd1*−/− and *Pkd2*−/− mice (12, 13, 20, 21, 24–26). Recent *in vitro* experiments have demonstrated that translocation of polycystin-2 to the plasma membrane requires polycystin-1 and that their coassembly produces calcium-permeable nonselective cation currents (8). Taken together, our data support the hypothesis that a complex of polycystin-1 and polycystin-2 at the cell membrane is required for further tubule development, and its absence results in cyst formation.

The mechanisms by which cysts arise in the kidney in ADPKD are unknown. Evidence from mutation analysis of cystic epithelial cells derived from adult cystic kidneys and from *Pkd1*−/− and *Pkd2*−/− mice strongly supports a two-hit mechanism involving somatic mutation at the *Pkd1* or *Pkd2* locus (41, 42). Although the loss of polycystin-1 function clearly leads to cyst formation, there is some evidence that altered levels of the protein may be pathogenic with elevated levels of polycystin-1 being associated with cyst formation in a mouse model carrying a human *PKD1* transgene (28). Cyst formation therefore may result from more complex mechanisms than somatic mutation alone. The early onset and relatively high frequency of microscopic cyst formation seen in ADPKD, where microscopic cysts have been detected very early in the course of the disease by renal biopsy (43), also suggest that mechanisms other than somatic mutation may be involved in the initiation of cyst formation. Indeed, the presence of microscopic cysts in *Pkd1*$^{del17–21\beta geo}$ heterozygotes from 3 months of age, affecting 1–2% of tubular cross sections would be consistent with this hypothesis. Subsequent somatic *Pkd1* mutation or other genetic or environmental effects then might be involved in cyst progression. Our mouse model therefore will be useful in addressing this question.

One of the major sites of *Pkd1* expression is in the developing and mature cardiovascular system. High levels of expression were detected in vascular smooth muscle and endothelial cells as well as in cardiac valves and myocytes. This expression pattern corresponds with the phenotype of *Pkd1*$^{del17–21\beta geo}$ −/− mice, which exhibit gross edema, s.c. hemorrhage, and structural cardiac defects. The atrial and ventricular septal abnormalities seen in *Pkd1*$^{del17–21\beta geo}$ −/− mice, including a common atrioventricular canal, have also been described in ≈50% of *Pkd2*−/− embryos (27), suggesting that *Pkd1* and *Pkd2* interact during cardiac development. Additional cardiovascular abnormalities, notably the DORV, seen in the *Pkd1*$^{del17–21\beta geo}$ −/− embryos are similar to those described in mice with neural crest defects (44, 45). Given that *Pkd1* was expressed throughout the heart, the presence of myocardial abnormalities and/or DORV in different *Pkd1*$^{del17–21\beta geo}$ −/− embryos was consistent with primary defects in both the myocardium and in neural crest-derived tissues in addition to possible secondary effects resulting from their interaction. The valvular abnormalities such as mitral valve prolapse seen in 25% of cases of ADPKD can now be explained readily by the demonstration of *Pkd1* expression in these developing structures (Fig. 3*f*). These expression data also suggest that a primary defect in vascular endothelial and/or smooth muscle cell function may be the cause of hypertension in ADPKD, independent of alterations in renal function. *Pkd1* expression in the afferent arteriole (Fig. 2*e*) would also support this hypothesis. Similarly, intracranial aneurysm formation may reflect a primary defect in vascular structure.

X-Gal staining of embryonic and adult tissues from *Pkd1*$^{del17–21\beta geo}$ heterozygote mice showed that *Pkd1* has a complex developmental and tissue-specific expression pattern (Figs. 2 and 3; unpublished data). These data point to a role for polycystin-1 in the development and physiology of a wide variety of different organ systems in addition to the kidney. Such a widespread role was not predicted from the pathology

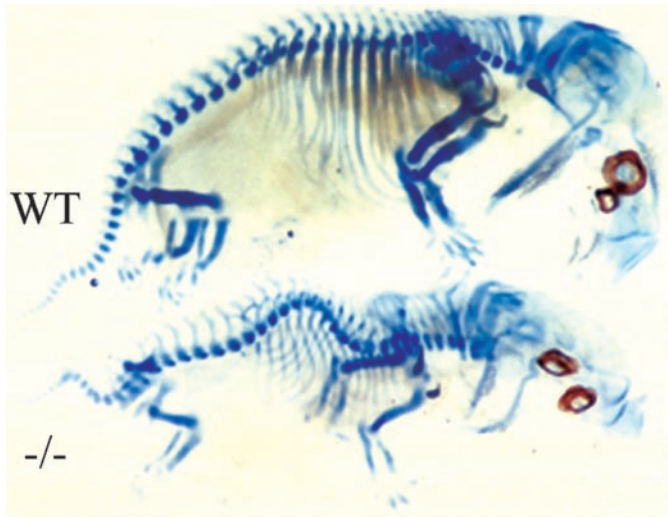

Fig. 5. Abnormal skeletal development in *Pkd1*$^{del17–21\beta geo}$ −/− mice. Cartilage staining of skeletal preparations from an E13.5 *Pkd1*$^{del17–21\beta geo}$ −/− embryo and WT (+/+) littermate showing abnormalities in cranial, facial, axial, and long bone formation in the mutant.

of ADPKD. *Pkd1*$^{del17–21\beta geo}$ $-/-$ mice have revealed that *Pkd1* is involved in bone formation; developing and mature cartilage are a major site of *Pkd1* expression, and skeletal development was severely disrupted in *Pkd1*$^{del17–21\beta geo}$ homozygote embryos (Fig. 5). Differences in the expression of *Pkd1* and *Pkd2* (21) and in *Pkd1* and *Pkd2* mutant mice also suggest novel tissue-specific functions for polycystin-1 that are independent of polycystin-2. For example in contrast to *Pkd1*, neural crest cell-derived tissues display low-to-undetectable *Pkd2* expression, which would explain the phenotypic differences between *Pkd1*$^{del17–21\beta geo}$ and *Pkd2* mutant mice (21, 27). Thus, polycystin-1 is likely to be a multifunctional protein involved in the development of a variety of tissues including the kidney, liver, pancreas, cardiovascular system, and skeleton. The characterization of mutant mice with different targeted mutations in *Pkd1* will help to elucidate these roles and determine whether, and if so how, the site of mutation in *Pkd1* influences the disease phenotype.

We thank Barbara Sgotto for technical help in preparing the targeting construct, Dipa Natarajan for initial screening of the genomic library, and Val Wilson for helpful discussions. This work was supported by a Wellcome Trust Senior Clinical Fellowship (awarded to R.S.) and an NKRF/Amgen training fellowship (awarded to S.M.). C.B. is a National Kidney Research Fund Senior Fellow and formerly a Lister Institute Research Fellow. Support was also provided by the Charities Committee (Addenbrooke's Hospital, Cambridge, UK) and the British Heart Foundation.

1. Murcia, N. S., Sweeney, W. E., Jr. & Avner, E. D. (1999) *Kidney Int.* **55,** 1187–1197.
2. Calvet, J. P. (1993) *Kidney Int.* **43,** 101–108.
3. Grantham, J. J. (1996) *Am. J. Kidney Dis.* **28,** 788–803.
4. Richards, W. G., Sweeney, W. E., Yoder, B. K., Wilkinson, J. E., Woychik, R. P. & Avner, E. D. (1998) *J. Clin. Invest.* **101,** 935–939.
5. Carone, F. A., Butkowski, R. J., Nakamura, S., Polenakovic, M. & Kanwar, Y. S. (1994) *Kidney Int.* **46,** 1368–1374.
6. Mochizuki, T., Wu, G., Hayashi, T., Xenophontos, S. L., Veldhuisen, B., Saris, J. J., Reynolds, D. M., Cai, Y., Gabow, P. A., Pierides, A. *et al.* (1996) *Science* **272,** 1339–1342.
7. Hughes, J., Ward, C. J., Peral, B., Aspinwall, R., Clark, K., Sanmillan, J. L., Gamble, V. & Harris, P. C. (1995) *Nat. Genet.* **10,** 151–160.
8. Hanaoka, K., Qian, F., Boletta, A., Bhunia, A. K., Piontek, K., Tsiokas, L., Sukhatme, V. P., Guggino, W. B. & Germino, G. G. (2000) *Nature (London)* **408,** 990–994.
9. Kim, E., Arnould, T., Sellin, L. K., Benzing, T., Fan, M. J., Gruning, W., Sokol, S. Y., Drummond, I. & Walz, G. (1999) *J. Biol. Chem.* **274,** 4947–4953.
10. Arnould, T., Kim, E., Tsiokas, L., Jochimsen, F., Gruning, W., Chang, J. D. & Walz, G. (1998) *J. Biol. Chem.* **273,** 6013–6018.
11. Boletta, A., Qian, F., Onuchic, L. F., Bhunia, A. K., Phakdeekitcharoen, B., Hanaoka, K., Guggino, W., Monaco, L. & Germino, G. G. (2000) *Mol. Cell.* **6,** 1267–1273.
12. Foggensteiner, L., Bevan, A. P., Thomas, R., Coleman, N., Boulter, C., Bradley, J., Ibraghimov-Beskrovnaya, O., Klinger, K. & Sandford, R. (2000) *J. Am. Soc. Nephrol.* **11,** 814–827.
13. Markowitz, G. S., Cai, Y., Li, L., Wu, G., Ward, L. C., Somlo, S. & D'Agati, V. D. (1999) *Am. J. Physiol.* **277,** F17–F25.
14. Torres, V. E., Cai, Y., Chen, X., Wu, G. Q., Geng, L., Cleghorn, K. A., Johnson, C. M. & Somlo, S. (2001) *J. Am. Soc. Nephrol.* **12,** 1–9.
15. Geng, L., Segal, Y., Peissel, B., Deng, N., Pei, Y., Carone, F., Rennke, H. G., Glucksmann-Kuis, A. M., Schneider, M. C., Ericsson, M., Reeders, S. T. & Zhou, J. (1996) *J. Clin. Invest.* **98,** 2674–2682.
16. Griffin, M. D., Torres, V. E., Grande, J. P. & Kumar, R. (1997) *J. Am. Soc. Nephrol.* **8,** 616–626.
17. Ibraghimov-Beskrovnaya, O., Dackowski, W. R., Foggensteiner, L., Coleman, N., Thiru, S., Petry, L. R., Burn, T. C., Connors, T. D., Van Raay, T., Bradley, J., *et al.* (1997) *Proc. Natl. Acad. Sci. USA* **94,** 6397–6402.
18. Palsson, R., Sharma, C. P., Kim, K., McLaughlin, M., Brown, D. & Arnaout, M. A. (1996) *Mol. Med.* **2,** 702–711.
19. Peters, D. J., Spruit, L., Klingel, R., Prins, F., Baelde, H. J., Giordano, P. C., Bernini, L. F., de Heer, E., Breuning, M. H. & Bruijn, J. A. (1996) *Lab. Invest.* **75,** 221–230.
20. Guillaume, R., D'Agati, V., Daoust, M. & Trudel, M. (1999) *Dev. Dyn.* **214,** 337–348.
21. Guillaume, R. & Trudel, M. (2000) *Mech. Dev.* **93,** 179–183.
22. Ward, C. J., Turley, H., Ong, A. C., Comley, M., Biddolph, S., Chetty, R., Ratcliffe, P. J., Gattner, K. & Harris, P. C. (1996) *Proc. Natl. Acad. Sci. USA* **93,** 1524–1528.
23. Van Adelsberg, J., Chamberlain, S. & D'Agati, V. (1997) *Am. J. Physiol.* **272,** F602–F609.
24. Kim, K., Drummond, I., Ibraghimov-Beskrovnaya, O., Klinger, K. & Arnaout, M. A. (2000) *Proc. Natl. Acad. Sci. USA* **97,** 1731–1736. (First Published February 4, 2000; 10.1073/pnas.040550097)
25. Lu, W., Peissel, B., Babakhanlou, H., Pavlova, A., Geng, L., Fan, X., Larson, C., Brent, G. & Zhou, J. (1997) *Nat. Genet.* **17,** 179–181.
26. Wu, G. Q., Dagati, V., Cai, Y. Q., Markowitz, G., Park, J. H., Reynolds, D. M., Maeda, Y., Le, T. C., Hou, H., Kucherlapati, R., Edelmann, W. & Somlo, S. (1998) *Cell* **93,** 177–188.
27. Wu, G., Markowitz, G. S., Li, L., D'Agati, V. D., Factor, S. M., Geng, L., Tibara, S., Tuchman, J., Cai, Y., Hoon Park, J., *et al.* (2000) *Nat. Genet.* **24,** 75–78.
28. Pritchard, L., Sloane-Stanley, J. A., Sharpe, J. A., Aspinwall, R., Lu, W., Buckle, V., Strmecki, L., Walker, D., Ward, C. J., Alpers, C. E., *et al.* (2000) *Hum. Mol. Genet.* **9,** 2617–2627.
29. Mountford, P., Zevnik, B., Duwel, A., Nichols, J., Li, M., Dani, C., Robertson, M., Chambers, I. & Smith, A. (1994) *Proc. Natl. Acad. Sci. USA* **91,** 4303–4307.
30. Bradley, A. (1987) in *Teratocarcinoms and embryonic stem cells. A practical approach.*, ed. Robertson, E. J. (IRL, Oxford), pp. 113–151.
31. Chomczynski, P. & Sacchi, N. (1987) *Anal. Biochem.* **162,** 156–159.
32. Hogan, B., Beddington, R., Costantini, F. & Lacy, E. (1994) *Manipulating the mouse embryo. A laboratory manual.* (Cold Spring Harbor Lab. Press, Plainview, NY).
33. Rossetti, S., Strmecki, L., Gamble, V., Burton, S., Sneddon, V., Peral, B., Roy, S., Bakkaloglu, A., Komel, R., Winearls, C. G. & Harris, P. C. (2001) *Am. J. Hum. Genet.* **68,** 46–63.
34. Torres, V. E. (1999) *Am. J. Kidney Dis.* **34,** xlv-xlviii.
35. Somlo, S., Rutecki, G., Giuffra, L. A., Reeders, S. T., Cugino, A. & Whittier, F. C. (1993) *J. Am. Soc. Nephrol.* **4,** 1371–1378.
36. Nauta, J., Goedbloed, M. A., van den Ouweland, A. M., Nellist, M. & Hoogeveen, A. T. (2000) *Histochem. Cell Biol.* **113,** 303–11.
37. Ong, A. C., Harris, P. C., Davies, D. R., Pritchard, L., Rossetti, S., Biddolph, S., Vaux, D. J., Migone, N. & Ward, C. J. (1999) *Kidney Int.* **56,** 1324–1333.
38. Peters, D. J., van de Wal, A., Spruit, L., Saris, J. J., Breuning, M. H., Bruijn, J. A. & de Heer, E. (1999) *J. Pathol.* **188,** 439–446.
39. Griffin, M. D., Osullivan, D. A., Torres, V. E., Grande, J. P., Kanwar, Y. S. & Kumar, R. (1997) *Kidney Int.* **52,** 1196–1205.
40. Van Adelsberg, J. (1999) *Dev. Genet.* **24,** 299–308.
41. Watnick, T. J., Torres, V. E., Gandolph, M. A., Qian, F., Onuchic, L. F., Klinger, K. W., Landes, G. & Germino, G. G. (1998) *Mol. Cell.* **2,** 247–251.
42. Watnick, T., He, N., Wang, K., Liang, Y., Parfrey, P., Hefferton, D., St. George-Hyslop, P., Germino, G. & Pei, Y. (2000) *Nat. Genet.* **25,** 143–144.
43. Torra, R., Badenas, C., Darnell, A., Bru, C., Escorsell, A. & Estivill, X. (1997) *Kidney Int.* **52,** 33–38.
44. Chien, K. R. (2000) *Nature (London)* **407,** 227–232.
45. Jacks, T., Shih, T. S., Schmitt, E. M., Bronson, R. T., Bernards, A. & Weinberg, R. A. (1994) *Nat. Genet.* **7,** 353–361.